The Variable Observer (Vol. 1): Multicolor (BVI_C) Light Curves and Period Analysis of the Eclipsing Binary IL Cnc

Kevin B. Alton[1,2]

[1] *UnderOak Observatory, Cedar Knolls, NJ, USA*
[2] *Desert Bloom Observatory, Benson, AZ, USA*

January 21, 2018

IL Cnc (Vmag=12.6) was first reported to be a W UMa-type variable star by Rinner et al. (2003) based on unfiltered ccd data. Photometric data had also been collected from this system during the ROTSE-I survey (NSVS; Woźniak et al. 2004) and later captured by the ASAS Survey (Pojmański et al. 2005). Sparsely sampled lightcurve data acquired over this time span (1999-2005) were folded by period analysis. This report also describes results from the first multicolor (BVI_c) ccd-based photometric study conducted on this variable target. The analysis of eclipse time differences (ETD) calculated from times-of-minima published in the literature and new data presented herein has resulted in a revised ephemeris for IL Cnc.

1 Methods

Time-series images were taken (90-sec) in 2014 with an SBIG ST-8XME CCD camera mounted at the Cassegrain focus of a 0.28-m catadioptric telescope. This f/6.4 instrument located in UnderOak Observatory (UO; NJ, USA) produces an image scale of 2.06 arcsec/pixel (bin=2×2) and a field-of-view (FOV) of $17.5' \times 26.3'$. Image acquisition (lights, darks, and flats) at UO was performed as described elsewhere (Alton 2016) and produced at least 282 values in each bandpass (B,V and I_c). Similarly at Desert Bloom Observatory (DBO; AZ, USA), an SBIG STT-1603ME CCD camera mounted at the Cassegrain focus of a 0.4-m catadioptric telescope was used for imaging IL Cnc in 2018. This f/6.8 instrument produces an image scale of 1.36 arcsec/pixel (bin=2×2) and a FOV of $11.5' \times 17.2'$. At DBO, image acquisition (75-sec) was performed using MaxIm DL Version 6.13 (Diffraction Limited) or TheSkyX Version 10.5.0 (Software Bisque). This most recent imaging campaign produced at least 235 individual photometric values in each bandpass. Both ccd cameras were equipped with B, V and I_c filters manufactured to match the Johnson-Cousins-Bessell prescription. Calibration and registration of all images collected at UO and DBO were performed with AIP4Win v2.4.0 (Berry and Burnell 2005). Instrumental readings were reduced to catalog-based magnitudes using the reference MPOSC3 star fields (Warner 2007) built into MPO Canopus v10.7.1.3 (Minor Planet Observer). The 2014 and 2018 lightcurves (LC) used an identical ensemble of five non-varying comparison stars in the same FOV. The identity, J2000 coordinates and color index (B-V) of these stars are listed in Table 1. Only data from images taken above 30° altitude (airmass <2.0) were accepted in order to minimize error due to differential refraction and color extinction.

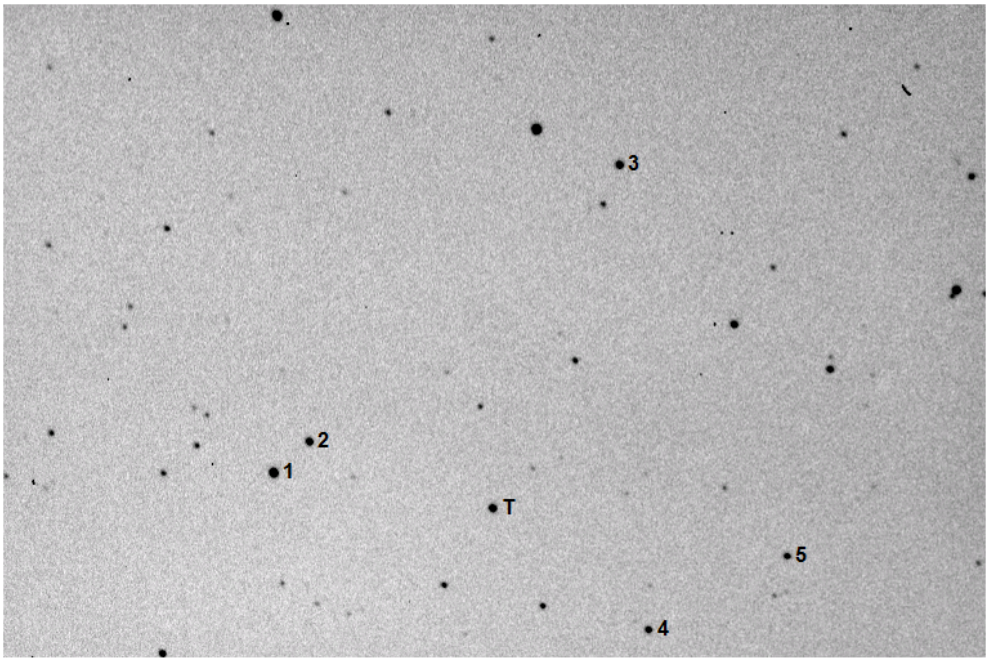

Figure 1: *Observed field-of-view for IL Cnc (T) obtained at UO. The comparison stars are marked according to the numbers (1-5) assigned in Table 1.*

2 Results and Discussion

Table 1. FOV identity, name, coordinates and color index (B-V) for the target (T) and comparison stars (1-5) used for ensemble aperture photometry

FOV Identity	Name	$\alpha_{2000.0}$ hh:mm:ss	$\delta_{2000.0}$ deg ′ ″	MPOSC3 (B-V)
1	GSC 01400-0523	08 56 04.26	+20 00 08.2	0.560
2	GSC 01400-0279	08 56 04.97	+20 01 06.8	0.711
3	GSC 01400-0330	08 56 11.63	+20 09 37.5	0.652
4	GSC 01400-0161	08 55 35.04	+20 05 05.6	0.588
5	GSC 01400-0406	08 55 34.19	+20 08 21.6	0.557
T	IL Cnc	08 55 51.51	+20 03 38.6	0.983

Sparsely sampled LC data from the ROTSE-I (1999-2000) and ASAS surveys (2002-2005) were adjusted to the same average magnitude and subjected to period analysis using the ANOVA routine proposed by Schwarzenberg-Czerny (1996) and implemented within Peranso v2.5 (CBA Belgium Observatory ©2011). The period-folded ($P = 0.267656 \pm 0.000009\ d$) results (Figure 2) indicate that significant differences in the brightness at maximum and minimum light can occur.

Photometric data from 2014 (Figure 3) and 2018 (Figure 4) could be folded using an identical period solution ($0.267656 \pm 0.000001\ d$) derived by Fourier analysis (FALC; Harris *et al.* 1989). This period was independently verified using ANOVA (Schwarzenberg-Czerny 1996). New times-of-minimum (ToM) were calculated using the method of Kwee and van Woerden (1956). A mean ToM value was calculated for each nighttime session since no obvious color dependency (BVI$_c$) was observed. These are summarized in Table 2 along with other published ToM values dating back from 2003. Cycle number and ETD values were calculated from the reference ephemeris (Rinner *et al.* 2003) where:

$$HJD_0 = 2452721.5705 + 0.26765 \times E.$$

Regression analysis of the ETD values calculated from all the observed and predicted minimum times versus the period cycle number produced a straight-line relationship indicating that the orbital period for this system does not appear to have substantively changed since 2003 (Figure 5). These data lead to the following revised linear

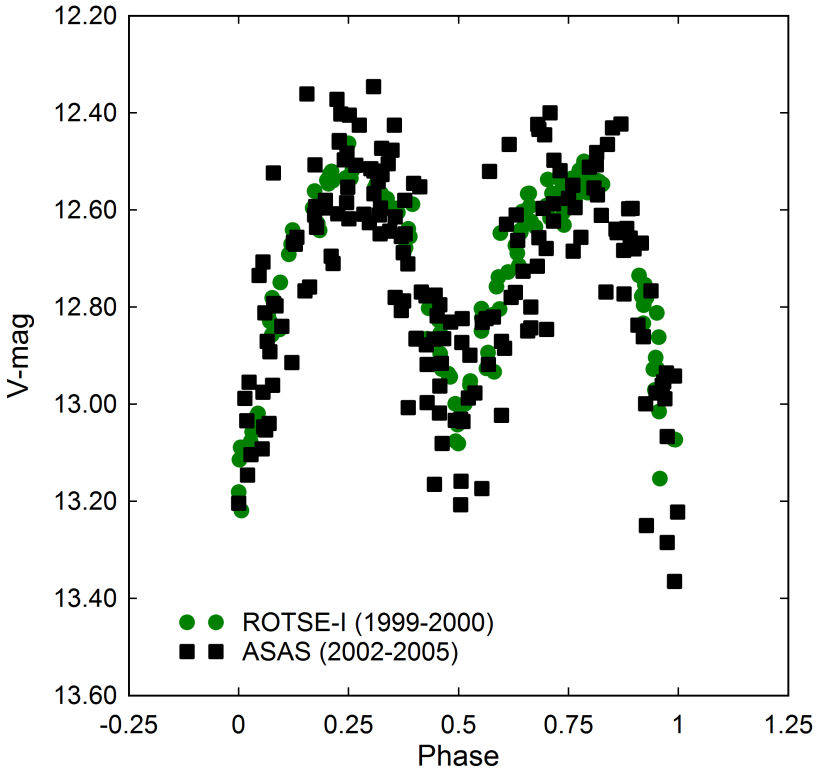

Figure 2: *Folded ($P = 0.267656 \pm 0.000009\ d$) light curves (V-mag) for IL Cnc produced from the ROTSE-I and ASAS Surveys*

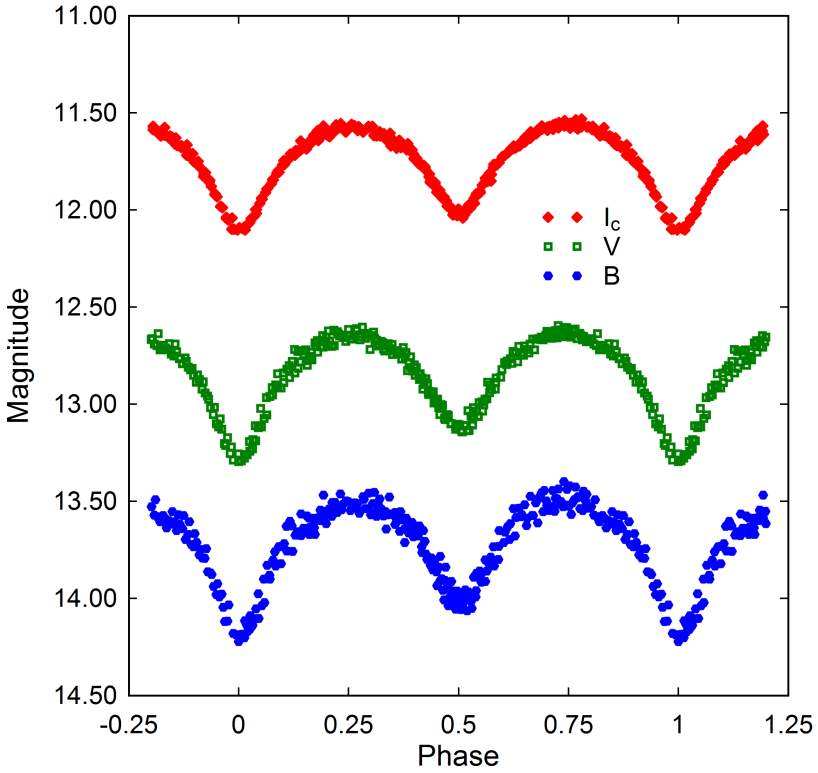

Figure 3: *Folded ($P = 0.267656 \pm 0.000001\ d$) light curves ($BVI_c$) for IL Cnc produced at UnderOak Observatory in 2014*

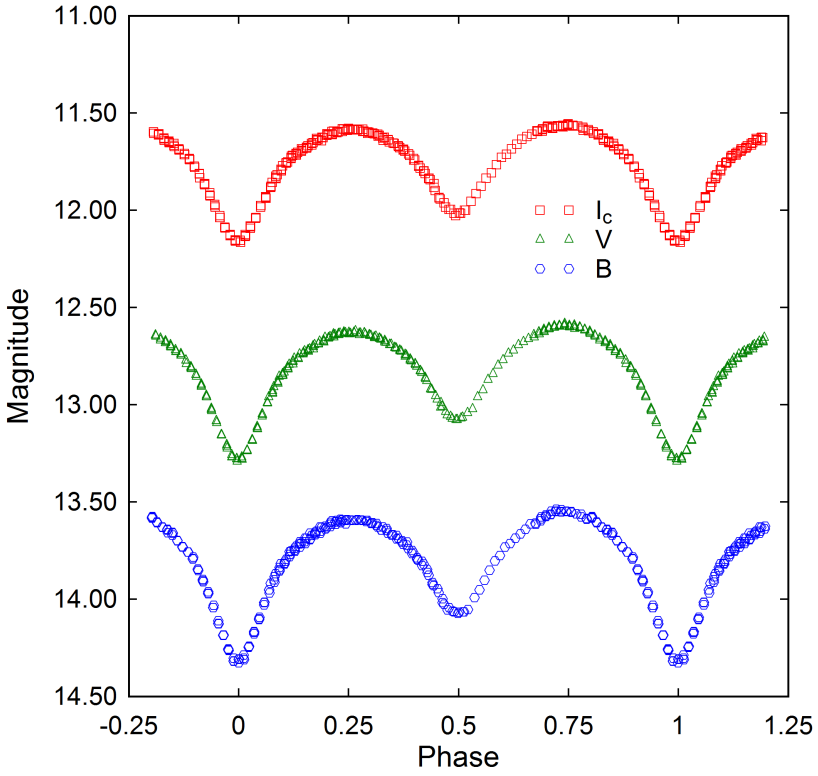

Figure 4: *Folded* ($P = 0.267656 \pm 0.000001\ d$) *light curves* ($BV\,I_c$) *for IL Cnc produced at Desert Bloom Observatory in 2018*

ephemeris:

$$HJD = 2458131.9657(10) + 0.2676559(1) \times E.$$

Since all but the first value represents data collected over a relative short time span ($\approx 10\ y$), it is far too early to establish whether some underlying periodicity may remain hidden in the data. Additional ToMs could prove very helpful to more thoroughly examine the secular behavior of this system.

The multicolor LCs (BVI$_c$) for IL Cnc shown in Figure 3 (2014) and Figure 4 (2018) reveal that minima are separated by 0.5 phase as would expected for an eclipsing binary star tidally locked in a circular orbit. The 2018 LCs exhibit peak asymmetry during maximum light such that Max II>Max I whereas not as much difference was observed at quadrature in 2014. This behavior, also called the O'Connell effect (O'Connell 1951), is generally attributed to hot or cold spots which can be large enough to affect the brightness in localized regions of either star. LC data collected from IL Cnc during the ASAS Survey dramatically illustrate this effect particularly during Min I and Max II (Figure 2). W UMa-type overcontact systems are well known to be photospherically active and from year-to-year can show large differences in maximum and minimum light. No classification spectrum is available for IL Cnc, however an estimate from (B-V) and (V-I$_c$) color index data generated from the new LCs herein and those reported by four other surveys (USNO-B1, 2MASS, SDSS-DR9 and UCAC4) cataloged in VizieR (Lasker *et al.* 1996) suggests that it is an early K type system. Additional spectroscopic data will be required to unequivocally classify this system. Attempts to model these data with PHOEBE 0.31a (Prŝa and Zwitter 2005), a GUI front-end to the Wilson-Devinney code (Wilson and Devinney 1971), failed to produce a unique solution for the mass-ratio since IL Cnc only exhibits a partial eclipse ($i \approx 74°$). As such any photometric solution will suffer from degeneracy while trying to simultaneously optimize orbital inclination (i) and mass-ratio (q_{ph}) unless there is a total eclipse (Terrell and Wilson 2005). This behavior is manifestly illustrated (Figure 6) during an exercise often called "q-search" or grid search to find a best value for the mass-ratio. Essentially q is incrementally changed within a fixed interval during Roche modeling while the orbital inclination (i), surface potential of the primary (Ω_1) and effective temperature of the secondary (T_2) are allowed to vary during optimization by differential corrections to minimize χ^2. As can be seen in Fig. 6 there is essentially no meaningful difference in the curve fits when q_{ph} varies between 1.5 and 2. In this case it is evident that radial velocity data will be necessary to produce an accurate mass-ratio and Roche model for IL Cnc.

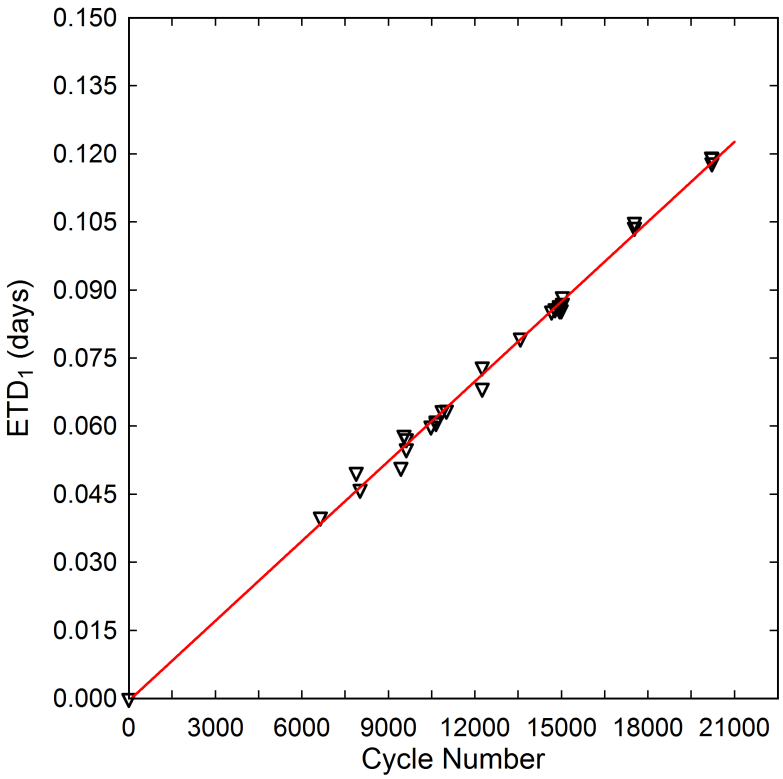

Figure 5: *Linear ephemeris* $(P = 0.2676559 \pm 0.0000001d)$ *for IL Cnc determined from eclipse timing differences observed between 2003 and 2018*

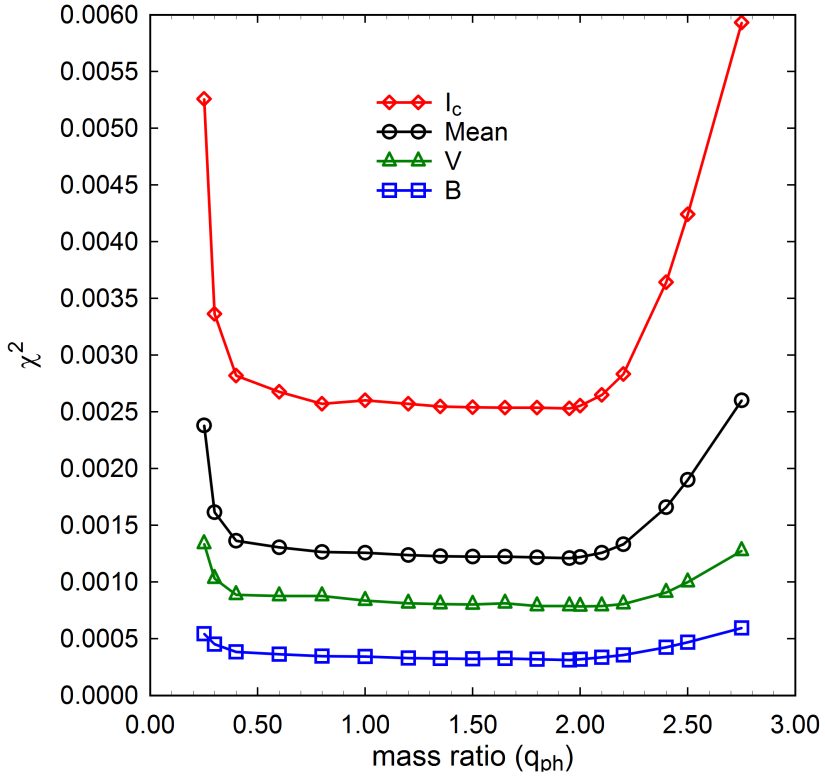

Figure 6: *Results from q-search illustrating failure to find a unique value for the photometric mass-ratio (q_{ph}) where the best LC model fit reaches a distinct minimum error (χ^2)*

Table 2. Eclipse time differences (ETD) calculated from published times-of-minimum for IL Cnc along with eight new values reported for the first time in this study

HJD (ToM) -2400000	Error	ETD	Cycle Number	Minimum type	Reference
52721.5705	-	0.000	0	primary	Rinner *et al.* 2003
54500.4124	0.0004	0.04000	6646	primary	Hübscher *et al.* 2010
54831.9068	0.0009	0.04987	7884.5	secondary	Diethelm 2009
54866.4299	0.0003	0.04613	8013.5	secondary	Hübscher and Monninger 2011
55245.8286	0.0009	0.05095	9431	primary	Diethelm 2010
55275.4110	0.0013	0.05802	9541.5	secondary	Hübscher and Monninger 2011
55295.3479	0.0010	0.05500	9616	primary	Hübscher and Monninger 2011
55295.4840	0.0009	0.05727	9616.5	secondary	Hübscher and Monninger 2011
55523.9260	0.0002	0.06000	10470	primary	Nelson 2011
55571.8365	0.0003	0.06115	10649	primary	Diethelm 2011
55571.9700	0.0003	0.06083	10649.5	secondary	Diethelm 2011
55627.3762	0.0002	0.06347	10856.5	secondary	Hübscher and Lehmann 2012
55667.6576	0.0004	0.06355	11007	primary	Diethelm 2011
56000.6190	0.0040	0.06835	12251	primary	Diethelm 2012
56000.7575	0.0007	0.07302	12251.5	secondary	Diethelm 2012
56355.6678	0.0002	0.07943	13577.5	secondary	Nelson 2014
56643.5313	0.0001	0.08585	14653	primary	Hübscher 2014
56677.7910	0.0002	0.08585	14781	primary	Nelson 2015
56711.6489	0.0003	0.08602	14907.5	secondary	This study
56714.5936	0.0003	0.08656	14918.5	secondary	This study
56719.1427	0.0002	0.08559	14935.5	secondary	This study
56720.6151	0.0006	0.08594	14941	primary	This study
56732.5252	0.0005	0.08862	14985.5	secondary	This study
56743.3679	0.0011	0.08850	15026	primary	Hübscher and Lehmann 2015
56743.5003	0.0011	0.08707	15026.5	secondary	Hübscher and Lehmann 2015
57414.3818	0.0005	0.10385	17533	primary	Hübscher 2017
57414.5167	0.0007	0.10492	17533.5	secondary	Hübscher 2017
58129.8257	0.0002	0.11927	20206	primary	This study
58131.8318	0.0001	0.11802	20213.5	secondary	This study
58131.9667	0.0002	0.11910	20214	primary	This study

In summary, LC and eclipse timing data for IL Cnc has revealed a W UMa-type system in which the orbital period has not meaningfully changed since 1999. A preliminary classification of IL Cnc based solely on color index (B-V and V-I_c) suggests that the primary component is an early K-type star. A comparison of LCs produced from photometric data collected during the ROTSE-I and ASAS surveys along with those new data reported herein suggest that IL Cnc has an active photosphere like most other overcontact binary systems possessing a strong magnetic dynamo. Due to limitations imposed by only exhibiting a partial eclipse, it is not possible to derive a reliable photometric value for the mass-ratio (q_{ph}) for this system without supporting radial velocity data.

3 Acknowledgments

This research has made use of the SIMBAD and VizieR databases, operated at Centre de Données astronomiques de Strasbourg, France. In addition, the International Variable Star Index maintained by the AAVSO, the ASAS Catalogue of Variable Stars and the Northern Sky Variability Survey (ROTSE-I) were mined for valuable information. The diligence and dedication of all associated with these organizations is greatly appreciated.

References

[1] Alton, K.B. 2016, *AAVSO*, **44**, 87.

[2] Berry, R. and Burnell, J. 2005,*The Handbook of Astronomical Image Processing, 2nd Ed*, Richmond VA, Willmann-Bell.

[3] Diethelm, R. 2009, *I.B.V.S.*, **5959**.

[4] Diethelm, R. 2010, *I.B.V.S.*, **5945**.

[5] Diethelm, R. 2011, *I.B.V.S.*, **5992**.

[6] Diethelm, R. 2012, *I.B.V.S.*, **6029**.

[7] Harris, A.W., Young, J.W., Bowell, E., *et al.* 1989, *Icarus*, **77**, 171.

[8] Hübscher, J. 2014, *I.B.V.S*, **6118**.

[9] Hübscher, J. 2017, *I.B.V.S*, **6196**.

[10] Hübscher, J. and Lehmann, P.B. 2012, *I.B.V.S.*, **6026**.

[11] Hübscher, J. and Lehmann, P.B. 2015, *I.B.V.S.*, **6149**.

[12] Hübscher, J., Lehmann, P.B., Monninger, G., et al. 2010, *I.B.V.S*, **5918**.

[13] Hübscher, J. and Monninger, G. 2011, *I.B.V.S.*, **5871**.

[14] Hübscher, J. and Monninger, G. 2011, *I.B.V.S.*, **5871**.

[15] Kwee, K.K. and Woerden, H. van 1956, *B.A.N.*, **12**, 327.

[16] Lasker, B.M., Sturch, C.R., Lopez, C., *et al.* 1996, *VizieR Online Data Catalog, Version 1.1*.

[17] Nelson, R.H. 2011, *I.B.V.S.*, **5966**.

[18] Nelson, R.H. 2014, *I.B.V.S.*, **6092**.

[19] Nelson, R.H. 2015, *I.B.V.S.*, **6131**.

[20] O'Connell D.J.K. 1951, *Pub. Riverview College Obs.*, **2**, 85.

[21] Pojmański, G., Pilecki, B., Szczygiel, D. 2005,*Pub. Riverview College Obs.*, **55**, 275.

[22] Rinner, C., Starkey, D. Demeautis, Ch., *et al.* 2003, *I.B.V.S.*, **5428**.

[23] Schwarzenberg-Czerny, A. 1996, *Astrophys. J.*, **460**, L107.

[24] Terrell, D. and Wilson, R.E. 2005, *Astrophys. and Space Sci.*, **296**, 221.

[25] Vannmunster, T. 2006, *Peranso v2.5, Period Analysis Software*, CBA Belgium Observatory.

[26] Warner, B. 2007, *Minor Planet Bulletin*, **34**, 113.

[27] Woźniak, P.R., Vestrand, W.T. Akerlof, C.W., *et al.* 2005, *AJ*, **127**, 2436.